UNIVERSITÄTSMEDIZIN GÖTTINGEN UMG

Polarity-sensitive activation maps for the multifocal visual evoked potential

Shariful Islam[1], Dorothe A. Poggel[1], Michael B. Hoffmann[2], Peter Dechent[3], Hans Strasburger[1]
[1]Dept. Medical Psychology, U. Göttingen; [2]Dept. Ophthalmology, U. Magdeburg; [3]MR-Research in Neurology & Psychiatry, U. Göttingen
shariful@math.uni-goettingen.de — www.hans.strasburger.de

Introduction:

- The folding of early visual cortex leads to visual-field-dependent signal cancellation and degraded S/N ratio in the VEP. We present a simple yet effective analysis technique for mfVEP data, based on a template signal obtained iteratively from signals with equalized polarity.
- Relative amplitude and polarity for each visual field patch are shown in a dartboard activity map and juxtaposed to fMRI retinotopic mapping data of the same subjects to highlight mechanisms of signal cancellation in the mfVEP.

Methods:

- Activity ≡ Pearson's correlation between local signal and template.
- Borders of polarity reversal are seen as color change in these maps.
- V1 and V2 folding by fMRI ring/wedge retinotopic mapping.
- Stimuli precisely matched between mfVEP and fMRI.
- Stimuli designed to obey cortical magnification in a novel way.
- MfVEP activity maps and fMRI retinotopic maps juxtaposed for the same subject to assess the impact of cortical folding on the mfVEP.

Stimulus: Stimuli were designed to be directly comparable between mfVEP and fMRI by using the same ring radii which were constructed using an exponential function in a novel way to obey cortical magnification as described by an inverse linear function (Fig. 3). For fMRI this led to Matlab-created sequences of expanding contrast-reversing rings and rotating wedges (classical retinotopic mapping), shown via MRI-compatible goggles (VisuaStimDigital, Resonance Technology) by Presentation®. Goggles' visual field: 32°×24° / 800×600 Pixel. Stimulus outer diameter was 22.8°. MfVEP stimuli were presented on a 39.5×29.5 cm CRT computer screen at 36.5 cm distance. Stimulus diameter 29.5 cm resulting in again 22.8°.

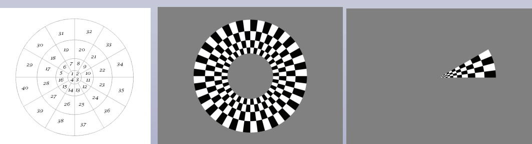

Fig. 1 . MVEP Visual Regions, Ring and Wedge

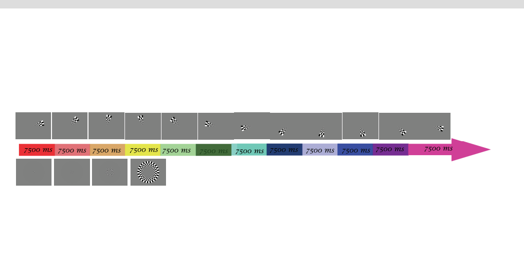

Fig. 2. Time course of a cycle of wedges and rings.

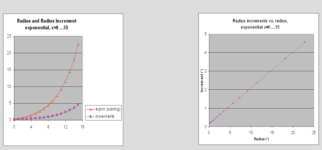

Fig. 3. The radius and radius increment function vs. ring index, and the radius increment function vs. radius

References
[1]Hood et al 2002, Quantifying the benefits of additional channels of multifocal VEP recording
[2]EEGLAB, Swartz Center for Computational Neuroscience , www.sccn.ucsd.edu/eeglab

Acknowledgements
Funded by DFG grant „Multifocal VEP and Cortex Folding“ (Str 354/7-1) to HS
We thank Michael Bach for help in mfVEP signal handling

Multifocal VEP (mfVEP):

❖ **Data acquisition and filtering:** mfVEP of four subjects were recorded on a VerisScience system in Magdeburg with reversal stimulation at 40 visual-field segments (Fig. 1). Electrodes were arranged in a "Southern Cross" on the inion (Hood[1] et al. 2002). Data were Fourier low-pass filtered at 40 Hz, i.e. linear trend was removed, the spectrum obtained from a DFT, data above 40 Hz cut off, and data back-transformed to obtain the smoothed signal. S/N ratio in all the four subjects was good (Fig. 4).

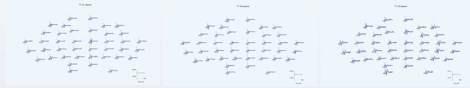

Fig. 4. Filtered Signals for Sj. TT in a Veris-like representation created with EEGLAB[2]

❖ **Template Creation:** An optimum template signal (Fig. 5) is created out of 120 signals obtained from three electrodes OL, OZ, OR for the first experiment with subject JT. The following algorithm was implemented in MATLAB to obtain the template signal:

1) Hand-pick the first signal as a seed for the template signal. Call it $S_1=S_{tem}$.
2) For all remaining signals, calculate the correlation r_i with the current best template signal S_{tem}. Choose the signal S_i with the highest $|r_i|$.
3) Add or subtract that signal S_i to the current best template signal S_{tem} depending on the sign of correlation. Remove S_i from the set of remaining signals.
4) Repeat Steps 2 and 3 until $|r_i|$ drops below a preset criterion, e.g. 0.6.
5) Divide S_{tem} by n, where n is the number of signals in (4).

This is the final template we obtained for subject TT:

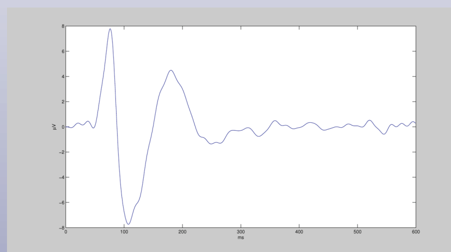

Fig. 5. Template Signal

❖ **Activity Map Creation:** Activity maps display the correlation between local signal and template (in the first 200 ms). Maximum and minimum correlation patches have white outlines.

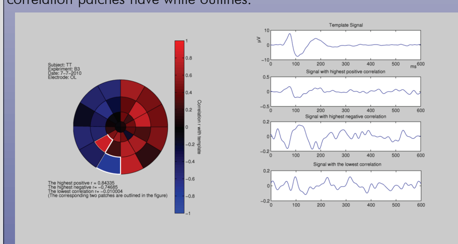

Fig. 6. Activity map for Sj. TT (electrode OL) in the second experiment

❖ **Average Activity Map Creation:** Three measurements for each subject. Average maps obtained from averaged signals. Correlation coefficients' standard deviation with forward/backward Fisher's Z-transform.

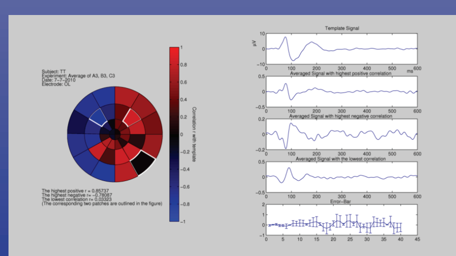

Fig. 7. Averaged activity map for Sj. TT (electrode OL) in three experiments

fMRI and mfVEP Activation Map:

Siemens Trio 3T MRI scanner (GE-EPI, TR=2500, 28 slices, 2×2×2 mm³ voxels, 5 wedge cycles, 10 ring cycles). A high-resolution anatomical scan (T1-weighted) was acquired for segmentation of the white-gray matter border. Retinotopic stimulus patterns are shown in Fig. 2. Activation patches corresponding to mfVEP segments determined by ROI analysis.

To highlight principles of signal cancellation, fMRI and mfVEP activation maps are juxtaposed. We considered in particular patches where activation maps show interesting deviations from the regular pattern.

Fig. fMRI and mfVEP activation maps explaining signal cancellation.

Summary:

The polarity pattern in the activity map is in accordance with the following general patterns:

➢ Since the left and right hemifield are represented on different hemispheres, corresponding mfVEP polarity reversals were evident for *lateral* recording sites.

➢ As the upper and lower hemifield are represented on the ventral and dorsal portion of the calcarine fissure, mfVEP polarity reversals were evident between the upper and lower hemifield for the *central* recording sites.

➢ Deviations from this pattern are evident for both above characteristics. These are due to peculiar folding of the cortical representations of the corresponding visual field locations.

Conclusions:

➢ The analysis approach allows for an automated evaluation of polarity patterns of the mfVEP, resulting in a clear visualization of the respective patterns.

➢ The impact of individual cortical folding on mfVEPs can be assessed in a straightforward manner.

➢ A perspective is opened on refined mfVEP-based visual field mapping, which takes cortical convolution as a source of signal cancellation and drop-out into account.